Permeability of Acetic Acid Across Gel and Liquid-Crystalline Lipid Bilayers Conforms to Free-Surface-Area Theory

Tian-Xiang Xiang and Bradley D. Anderson
Department of Pharmaceutics and Pharmaceutical Chemistry, University of Utah, Salt Lake City, Utah 84112 USA

ABSTRACT Solubility-diffusion theory, which treats the lipid bilayer membrane as a bulk lipid solvent into which permeants must partition and diffuse across, fails to account for the effects of lipid bilayer chain order on the permeability coefficient of any given permeant. This study addresses the scaling factor that must be applied to predictions from solubility-diffusion theory to correct for chain ordering. The effects of bilayer chemical composition, temperature, and phase structure on the permeability coefficient (P_m) of acetic acid were investigated in large unilamellar vesicles by a combined method of NMR line broadening and dynamic light scattering. Permeability values were obtained in distearoylphosphatidylcholine, dipalmitoylphosphatidylcholine, dimyristoylphosphatidylcholine, and dilauroylphosphatidylcholine bilayers, and their mixtures with cholesterol, at various temperatures both above and below the gel → liquid-crystalline phase transition temperatures (T_m). A new scaling factor, the permeability decrement f, is introduced to account for the decrease in permeability coefficient from that predicted by solubility-diffusion theory owing to chain ordering in lipid bilayers. Values of f were obtained by division of the observed P_m by the permeability coefficient predicted from a bulk solubility-diffusion model. In liquid-crystalline phases, a strong correlaton ($r = 0.94$) between f and the normalized surface density σ was obtained: $\ln f = 5.3 - 10.6\sigma$. Activation energies (E_a) for the permeability of acetic acid decreased with decreasing phospholipid chain length and correlated with the sensitivity of chain ordering to temperature, $\partial\sigma/\partial(1/T)$, as chain length was varied. P_m values decreased abruptly at temperatures below the main phase transition temperatures in pure dipalmitoylphosphatidylcholine and dimyristoylphosphatidylcholine bilayers (30–60-fold) and below the pretransition in dipalmitoylphosphatidylcholine bilayers (8-fold), and the linear relationship between $\ln f$ and σ established for liquid-crystalline bilayers was no longer followed. However, in both gel and liquid-crystalline phases $\ln f$ was found to exhibit an inverse correlation with free surface area ($\ln f = -0.31 - 29.1/a_f$, where a_f is the average free area (in square angstroms) per lipid molecule). Thus, the lipid bilayer permeability of acetic acid can be predicted from the relevant chain-packing properties in the bilayer (free surface area), regardless of whether chain ordering is varied by changes in temperature, lipid chain length, cholesterol concentration, or bilayer phase structure, provided that temperature effects on permeant dehydration and diffusion and the chain-length effects on bilayer barrier thickness are properly taken into account.

INTRODUCTION

One of the major functions of biological membranes is to regulate the permeation of various chemical species into and out of cells. Passive permeation across lipid bilayers, a major component of biological membranes, occurs invariably for any chemical species driven by a gradient of the chemical potential and is the predominant mechanism by which most drug molecules reach their intended sites of action. Thus, understanding the physicochemical factors that govern molecular permeability across lipid bilayers is essential from the perspectives of both practical application and fundamental research.

The most commonly employed model for describing the passive transport of permeants across isolated lipid bilayers and transcellular permeation in biological membranes is the solubility-diffusion model, which relates a given solute's permeability coefficient to its ability to partition into and diffuse across the lipoidal membrane interior (Finkelstein, 1976; Walter and Gutknecht, 1986). As typically applied, however, solubility-diffusion theory is highly oversimplified and of little predictive value because it fails to take into account the diverse and complex properties of real bilayers and biomembranes. For example, lipid bilayer membranes that are known to be more "ordered" as a result of polar headgroup composition, chain length, or cholesterol concentration (Finkelstein, 1976; Lande et al., 1995; Sada et al., 1990; Todd et al., 1989a,b) or at temperatures below the gel-to-liquid-crystalline phase transition (Bar-On and Degani, 1985; Bresseleers et al., 1984; Magin and Niesman, 1984) or monolayers under high lateral pressures (Peters and Beck, 1983) have greater resistances to solute permeation, often by orders of magnitude. Lipid bilayer–water partition coefficients of small nonelectrolytes decrease significantly with increasing lipid surface density (DeYoung and Dill, 1988, 1990), and solutes distribute nonuniformly within bilayers (Marqusee and Dill, 1986; Subczynski and Hyde, 1983; Xiang and Anderson, 1994a). Solute permeation in lipid bilayers shows a much steeper dependence on permeant size than on diffusion in bulk solvents (Lieb and Stein, 1986; Xiang and Anderson, 1994b), and diffusion coefficients calculated from permeability coefficients are often orders of magnitude smaller than those obtained in bulk solvents. Although free volume has been shown to be

Received for publication 22 May 1996 and in final form 18 October 1996.
Address reprint requests to Dr. Bradley D. Anderson, Department of Pharmaceutics and Pharmaceutical Chemistry, University of Utah, 421 Wakara Way, Research Park, Salt Lake City, UT 84108-1210. Tel.: 801-581-4688; Fax: 801-585-3614; E-mail: banderson@deans.pharm.utah.edu.

0006-3495/97/01/223/15 $2.00

a critical variable in determining molecular diffusion and chemical potential in simple fluids and polymers (Hildebrand, 1977; Turnbull and Cohen, 1970; Vrentas, 1977) and has been speculated to play an important role in determining molecular permeability across biological membranes (Stein, 1986; Trauble, 1971), no quantitative relationships have been developed to support the latter hypothesis.

Biological membranes exhibit greater complexity than single-component bilayers, inasmuch as they comprise multiple lipid constituents and proteins. Nonideal mixing of different lipids within biological membranes may cause changes in phase structure and may result in the coexistence of two or more phase domains. Whereas most biological membranes exist in liquid-crystalline phases, many of the lipids isolated from stratum corneum (Lampe et al., 1983) and myelin (Barenholtz, 1984) exist mainly in their gel states at physiological temperature. Changes in bilayer chemical composition and phase structure can lead to changes in solute permeability.

One of the central objectives of transport studies in the authors' laboratories is to identify those physical variables in lipid membranes that play a dominant role in controlling solute permeability, given the complex physicochemical nature of biological membranes. Once these physical variables have been determined, the elucidation of various quantitative relationships capable of predicting solute permeability may follow. We recently proposed (Xiang and Anderson, 1995b) that chain ordering in lipid bilayers, which can be characterized by both segmental order parameters and bilayer surface density, is a major determinant of molecular transport across liquid-crystalline bilayers. This hypothesis was supported by the establishment of a quantitative relationship between the permeability coefficient for acetic acid and the surface density of dimyristoylphosphatidylcholine:cholesterol bilayers that vary in cholesterol concentration and temperature.

The present study extends the exploration of the relationship between the permeability of acetic acid and lipid chain packing within lipid bilayers to encompass the effects of phospholipid chain length, cholesterol concentration, temperature, and bilayer phase structure. We examine the hypothesis that the bilayer free-surface area is a "universal" variable that quantitatively relates solute permeability to chain packing in both liquid-crystalline and gel phases. To this end, we develop a relationship between the free-surface area, which can be calculated from experimental measurements (e.g., the order parameters), and the permeability coefficient of a model solute corrected for those factors assumed to be independent of chain packing (e.g., temperature dependence of permeant dehydration and diffusion and changes in barrier thickness with chain length). As in previous studies (Xiang and Anderson, 1995a,b), we measured the permeability coefficient for acetic acid in large unilamellar vesicles (LUVs), using a combined method of NMR line broadening and dynamic light scattering. This method was validated in a separate study by Xiang and Anderson (1995a), who explored the influences of permeant concentration, chemical shift reagent concentration, pD, ionic strength, vesicle size distribution, and different extrusion procedures for LUV preparation on permeability.

MATERIALS AND METHODS

Materials

Distearoylphosphatidylcholine (DSPC), dipalmitoylphosphatidylcholine (DPPC), dimyristoylphosphatidylcholine (DMPC), and dilauroylphosphatidylcholine (DLPC) were purchased from Avanti Polar Lipids, Inc. (Pelham, AL). Cholesterol (99+%) was purchased from Sigma Chemical Co. (St. Louis, MO). Acetic acid (99.8%) was purchased from Aldrich Chemical Co., Inc., (Milwaukee, WI). All other reagents were obtained commercially and were of analytical reagent grade. Polycarbonate membranes and membrane holders were obtained from Nuclepore, Inc. (Pleasanton, CA).

LUV liposome preparation

A detailed description of the experimental procedure has been published elsewhere (Xiang and Anderson, 1995a). In brief, LUVs were prepared by a modified combined technique that is due to Bangham et al. (1965) and Olson et al. (1979). Phospholipid (5–10 mg) and cholesterol (0–5 mg) were accurately weighed, dissolved in chloroform, rotary evaporated to a dry thin film on the bottom of a round-bottom flask at ≈40°C, and left under vacuum for 2 h at ≈50°C. An aqueous solution (≈1 mL) containing 5–50 mM acetic acid was then added, and the lipids were hydrated by repeated vortexing and shaking at a temperature above their main transition temperature. The multilamellar vesicles (MLVs) formed were forced through a 0.1 or 0.2 μm polycarbonate filter 17 times before the NMR transport experiments.

Determination of permeability coefficients across lipid bilayers

The internal lifetime for acetic acid in the phospholipid:cholesterol LUVs was determined as a function of phospholipid chain length (12–18), cholesterol composition (X_{chol} = 0.0–0.4), and temperature (10–65°C) by the ^{1}H-NMR line-broadening method originally developed by Alger and Prestegard (1979) and recently validated by Xiang and Anderson (1995a). LUVs were prepared in deuterated water as described above. The experiments were performed on a Bruker-200 NMR spectrometer (Bruker Instruments, Inc., Billerica, MA) operated in the Fourier-transform mode at 200 MHz. Samples were equilibrated for 20 min at a given temperature controlled by a standard variable-temperature accessory (BVT1000, Bruker). Each spectrum was the average of 32–1000 acquisitions separated by a pulse delay of 2–5 s. The spectra were Fourier transformed and phased with an ASPECT 3000 computer. The resonance frequencies of the methyl protons of acetic acid located inside and outside the vesicles, ω_i and ω_o, were separated by addition of a small amount of an impermeable shift reagent, $Pr(NO_3)_3$, to each LUV sample to attain a final concentration of 1–5 mM before the spectral acquisition. The effects of Pr^{+3} on the permeability of acetic acid were thoroughly explored in a separate study (Xiang and Anderson, 1995a). The permeability coefficient for acetic acid across DMPC:cholesterol (X_{chol} = 0.2) bilayers was found to be independent of $[Pr^{+3}]$ for $[Pr^{+3}] < 0.04$ M. (The actual concentration of free Pr^{+3} available for binding to the outer vesicle surface is lower than the 1–5 mM Pr^{+3} used in this study, as acetic acid in solution also forms complexes with Pr^{+3}. For example, at $[Pr^{+3}]$ = 0.005 M and a total acetic acid concentration of 0.05 M (pD = 6.32), only one quarter of the total Pr^{+3} would exist in the uncomplexed form.)

We obtained the lifetime of the permeant inside the vesicle, τ_i, by using the following linewidth expression in the slow-exchange limit,

$|\omega_i - \omega_o| T_{2,i} \gg 1$ (Piette and Anderson, 1959):

$$\pi\Delta\nu = 1/\tau_i + 1/T_{2,i}, \quad (1)$$

where $\Delta\nu$ is the full linewidth at one half of the maximum peak height and $T_{2,i}$ is the spin–spin relaxation time, which includes heterogeneous line broadening in the absence of exchange. The linewidth in the absence of exchange ($1/T_{2,i}$ = 2.6–5.0 Hz) was obtained at a low temperature, a high pD, or both, where the permeation rate is negligible. In gel-phase DPPC bilayers and at a permeant concentration > 0.03 M, the linewidth for acetic acid was found to increase with pD. The opposite trend was observed at a lower permeant concentration (≤0.008 M). Assuming that the bilayer is relatively impermeable to the ionized species (Xiang and Anderson, 1994c; Xiang et al., 1992), the abnormal pD dependence at a high permeant concentration may indicate alteration of bilayer chain packing at high acetate concentrations. Previous studies showed that addition of solutes to gel-phase DPPC bilayers may result in interdigitation to form the $L_{\beta i}$ phase (Simon and McIntosh, 1984). The permeability coefficients reported here for the gel-phase lipid bilayers were therefore obtained at a permeant concentration of <0.008 M to minimize the undesired effect of permeant on the bilayer properties.

The apparent permeability coefficient was calculated according to the following relationship:

$$P_{app} = \frac{V}{\tau_i A_t}, \quad (2)$$

where V is the entrapped volume and A_t is the vesicle surface area. The V/A_t ratio was determined from the hydrodynamic diameter d as obtained in dynamic light scattering measurements according to the formula

$$V/A_t = (d - \Delta r)/6, \quad (3)$$

where Δr is the bilayer thickness. Assuming a constant hydrocarbon density in the bilayer interior (even a drastic change in surface area (≈30%) at the main phase transition induces only a small change in the local density (≈4%) (Nagle and Wilkinson, 1978)), the bilayer thickness can be estimated from the relation

$$\Delta r = \delta_{hc} + \delta_{hg} = \frac{l_0 A_0}{A} + \delta_{hg} = l_0\sigma + \delta_{hg}, \quad (4)$$

where δ_{hc} and δ_{hg} are the thicknesses of the hydrocarbon and the headgroup regions, respectively, A is the area per lipid molecule, A_0 (40.8 Å^2) is the area per lipid molecule in the crystal, σ is the normalized surface density, and l_0 is the chain length in a bilayer in which all chains are fully aligned. l_0 can be calculated from known bond-length and angle parameters, which yield l_0 = 43.4, 38.4, 33.2, and 28.0 Å for DSPC, DPPC, DMPC, and DLPC bilayers, respectively. The σ values were obtained from the literature (see Table 1).

Dynamic light-scattering measurements were performed with a photon correlation spectrometer (Model BI-90, Brookhaven Instruments Co., Holtsville, NY) and a He–Ne laser light source at 632.8-nm wavelength. One drop of LUV suspension was placed in a 13 × 75 mm clean glass test tube and brought to a volume of 2 mL with the same filtered solution in the presence of 1–5 mM Pr^{3+} used to prepare the LUVs. The sample was placed in a temperature-controlled cuvette holder with a toluene index-matching bath. Autocorrelation functions were determined for a period of 100 s with a 10–80-μs duration at 90° and analyzed by the method of cumulants.

The bilayer membrane permeability coefficient for the neutral acetic acid molecule, P_m, was calculated from the apparent permeability coefficients obtained at a given pD by the following equation:

$$P_m = P_{app}\frac{([D^+] + K_a)}{[D^+]}, \quad (5)$$

where $K_a = 7.55 \times 10^{-6}$ is the dissociation constant for acetic acid in D_2O (Korman and LaMer, 1936). Eqation 5 assumes that the observed linewidth changes are due to permeation of un-ionized acetic acid, as verified in a previous study (Xiang and Anderson, 1995a).

RESULTS AND DISCUSSION

The most generally accepted model to describe the permeation of small neutral permeants across lipid bilayer membranes is the solubility-diffusion model (Finkelstein, 1976, 1987; Paula et al., 1996), which was originally applied by Overton (1896, 1899) and others (Collander, 1954; Collander and Barlund, 1933) to permeation across cell membranes. Solubility-diffusion theory depicts the bilayer membrane as a thin, homogeneous slab of bulk organic solvent into which the permeant must partition and diffuse across. Thus, the permeability coefficient, P_0, can be expressed as

$$P_0 = \frac{K_{hc/w} D_{hc}}{\delta_{hc}}, \quad (6)$$

where $K_{hc/w}$ is the partition coefficient of the permeant between water and a bulk organic solvent resembling the membrane interior (e.g., a liquid hydrocarbon) and D_{hc} is the diffusion coefficient of the permeant within the membrane, which is approximated by the diffusion coefficient of the permeant in a bulk hydrocarbon solvent (Finkelstein, 1976). The thickness of the hydrocarbon interior is given as δ_{hc}.

Finkelstein (1976) suggested that Eq. 6 might reasonably predict relative permeabilities of molecules that vary in structure but that absolute values of the permeability coefficients are "scaled by lipid composition." Noting that lower values of the permeability coefficient result from incorporation of cholesterol into lipid bilayers, from reduction of temperature, or from comparing sphingomyelin with lecithin, he suggested that "packing" of the lipid chains may reduce permeability coefficients through an increased viscosity (i.e., a reduction in diffusion coefficient) within the membrane, a "tightening of the membrane surface to penetration and solute accommodation" (i.e., reduction in partition coefficients into the membrane), or both. Which scaling factor should be used to account for such chain-ordering effects is a subject that has never been addressed quantitatively. It is clear from the above discussion that solubility-diffusion theory as typically employed (i.e., Eq. 6) neglects the role of lipid composition and temperature in permeabilities in lipid bilayers and therefore is of little value in predicting absolute permeabilities for any given permeant in any bilayer. This study seeks to define quantitatively the relationship among permeability of a single model permeant, acetic acid, and chain packing as altered by lipid chain length, lipid composition, or temperature, with the long-range goal of establishing a comprehensive model capable of predicting absolute permeability coefficients.

TABLE 1 Observed and corrected permeability coefficients for acetic acid across phospholipid:cholesterol LUVs as a function of temperature and cholesterol concentration

Lipid	X_{chol}	T (°C)	Phase	σ*	P_m (cm/s)	P_o (cm/s)#	f§
DLPC	0.2	21	L	0.688	$(4.4 \pm 0.5) \times 10^{-3}$¶	2.6×10^{-2}	1.7×10^{-1}
		25	L	0.676	$(6.6 \pm 0.6) \times 10^{-3}$¶	3.1×10^{-2}	2.1×10^{-1}
		30	L	0.663	$(8.4 \pm 0.5) \times 10^{-3}$¶	4.0×10^{-2}	2.1×10^{-1}
		35	L	0.649	$(1.2 \pm 0.1) \times 10^{-2}$¶	5.0×10^{-2}	2.4×10^{-1}
		45	L	0.621	$(2.6 \pm 0.3) \times 10^{-2}$¶	7.9×10^{-2}	3.3×10^{-1}
	0.4	21	L	0.841	$(1.1 \pm 0.2) \times 10^{-3}$¶	2.1×10^{-2}	5.3×10^{-2}
		25	L	0.823	$(1.4 \pm 0.2) \times 10^{-3}$¶	2.6×10^{-2}	5.5×10^{-2}
		30	L	0.800	$(2.1 \pm 0.4) \times 10^{-3}$¶	3.3×10^{-2}	6.4×10^{-2}
		35	L	0.781	$(3.3 \pm 0.3) \times 10^{-3}$¶	5.1×10^{-2}	6.5×10^{-2}
		40	L	0.762	$(4.1 \pm 0.5) \times 10^{-3}$¶	5.3×10^{-2}	7.8×10^{-2}
		45	L	0.743	$(7.1 \pm 0.8) \times 10^{-3}$¶	6.6×10^{-2}	1.1×10^{-1}
DMPC	0.0	20	G	0.818‖	$(3.9 \pm 0.5) \times 10^{-4}$¶	1.7×10^{-2}	2.3×10^{-2}
		26	L	0.613	$(6.5 \pm 0.6) \times 10^{-3}$¶**	3.0×10^{-2}	2.1×10^{-1}
		30	L	0.604	$(1.2 \pm 0.4) \times 10^{-2}$¶**	3.7×10^{-2}	3.3×10^{-1}
		33	L	0.595	$(1.3 \pm 0.3) \times 10^{-2}$¶**	4.2×10^{-2}	3.1×10^{-1}
		36	L	0.586	$(2.0 \pm 0.4) \times 10^{-2}$¶**	4.9×10^{-2}	4.1×10^{-1}
	0.2	21	G–L	0.787	$(9.1 \pm 0.8) \times 10^{-4}$¶**	1.9×10^{-2}	4.8×10^{-2}
		26	L	0.735	$(1.4 \pm 0.1) \times 10^{-3}$¶**	2.5×10^{-2}	5.5×10^{-2}
		30	L	0.700	$(2.4 \pm 0.2) \times 10^{-3}$¶**	3.2×10^{-2}	7.6×10^{-2}
		35	L	0.678	$(4.2 \pm 0.4) \times 10^{-3}$¶**	4.1×10^{-2}	1.0×10^{-1}
		40	L	0.660	$(9.4 \pm 1.0) \times 10^{-3}$¶**	5.1×10^{-2}	1.8×10^{-1}
	0.4	25	L	0.875	$(2.5 \pm 0.3) \times 10^{-4}$¶**	2.0×10^{-2}	1.2×10^{-2}
		30	L	0.855	$(4.8 \pm 0.4) \times 10^{-4}$¶**	2.6×10^{-2}	1.9×10^{-2}
		35	L	0.829	$(8.3 \pm 0.5) \times 10^{-4}$¶**	3.3×10^{-2}	2.5×10^{-2}
		40	L	0.797	$(1.5 \pm 0.1) \times 10^{-3}$¶**	4.2×10^{-2}	3.5×10^{-2}
		50	L	0.756	$(7.0 \pm 0.5) \times 10^{-3}$¶**	6.7×10^{-2}	1.1×10^{-1}
DPPC	0.0	25	G	0.895‖	$(1.7 \pm 0.5) \times 10^{-5}$¶	1.7×10^{-2}	9.9×10^{-4}
		30	G	0.873‖	$(2.7 \pm 0.6) \times 10^{-5}$##	2.2×10^{-2}	1.2×10^{-3}
		34	G	0.859‖	$(7.8 \pm 1.0) \times 10^{-5}$¶	2.7×10^{-2}	2.9×10^{-3}
		35	G	0.855‖	$(2.0 \pm 0.3) \times 10^{-4}$¶	2.8×10^{-2}	7.2×10^{-3}
		36	G	0.852‖	$(2.2 \pm 0.4) \times 10^{-4}$¶	2.9×10^{-2}	7.5×10^{-3}
		38	G	0.837‖	$(3.1 \pm 0.7) \times 10^{-4}$##	3.2×10^{-2}	9.6×10^{-3}
		40	G	0.825‖	$(7.1 \pm 0.7) \times 10^{-4}$¶	3.5×10^{-2}	2.0×10^{-2}
		41	L	0.671‖	$(6.6 \pm 0.6) \times 10^{-3}$¶	4.5×10^{-2}	1.5×10^{-1}
		43	L	0.638‖	$(9.3 \pm 0.8) \times 10^{-3}$##	5.2×10^{-2}	1.8×10^{-1}
		45	L	0.622	$(1.3 \pm 0.1) \times 10^{-2}$##	5.8×10^{-2}	2.3×10^{-1}
		50	L	0.604	$(3.3 \pm 0.4) \times 10^{-2}$¶	7.2×10^{-2}	4.6×10^{-1}
	0.2	30	G–L	0.880	$(3.3 \pm 0.3) \times 10^{-4}$¶	2.2×10^{-2}	1.5×10^{-2}
		35	G–L	0.824§§	$(5.5 \pm 0.6) \times 10^{-4}$¶	2.9×10^{-2}	1.9×10^{-2}
		40	L	0.760§§	$(1.5 \pm 0.2) \times 10^{-3}$¶	3.9×10^{-2}	3.9×10^{-2}
		45	L	0.695	$(4.5 \pm 0.5) \times 10^{-3}$¶	5.2×10^{-2}	8.7×10^{-2}
		50	L	0.670§§	$(9.4 \pm 1.0) \times 10^{-3}$¶	6.5×10^{-2}	1.5×10^{-1}
		55	L	0.655	$(2.2 \pm 0.2) \times 10^{-2}$¶	8.0×10^{-2}	2.7×10^{-1}
	0.4	30	L	0.885	$(2.5 \pm 0.2) \times 10^{-4}$¶	2.2×10^{-2}	1.2×10^{-2}
		35	L	0.863§§	$(5.0 \pm 0.6) \times 10^{-4}$¶	2.8×10^{-2}	1.8×10^{-2}
		40	L	0.841§§	$(6.8 \pm 0.6) \times 10^{-4}$¶	3.5×10^{-2}	2.0×10^{-2}
		45	L	0.819	$(1.2 \pm 0.1) \times 10^{-3}$¶	4.4×10^{-2}	2.8×10^{-2}
		50	L	0.795	$(3.3 \pm 0.4) \times 10^{-3}$¶	5.5×10^{-2}	6.0×10^{-2}
		55	L	0.773	$(6.0 \pm 0.6) \times 10^{-3}$¶	6.8×10^{-2}	8.8×10^{-2}
DSPC	0.2	40	G–L	0.873§§	$(1.6 \pm 0.2) \times 10^{-4}$¶	3.0×10^{-2}	5.4×10^{-3}
		45	G–L	0.877§§	$(4.0 \pm 0.6) \times 10^{-4}$¶	3.6×10^{-2}	1.1×10^{-2}
		50	G–L	0.863§§	$(1.6 \pm 0.3) \times 10^{-3}$##	4.5×10^{-2}	3.6×10^{-2}
		54	L	0.751§§	$(4.2 \pm 0.5) \times 10^{-3}$¶	6.0×10^{-2}	7.1×10^{-2}
		55	L	0.724§§	$(1.2 \pm 0.2) \times 10^{-2}$¶	6.4×10^{-2}	1.9×10^{-1}
		60	L	0.646§§	$(1.5 \pm 0.2) \times 10^{-2}$¶	8.6×10^{-2}	1.7×10^{-1}
		65	L	0.619§§	$(1.9 \pm 0.3) \times 10^{-2}$¶	1.1×10^{-1}	1.8×10^{-1}

TABLE 1—*Continued*

Lipid	X_{chol}	T (°C)	Phase	σ*	P_m (cm/s)	P_o (cm/s)#	f§
	0.4	40	G–L	0.862§§	$(2.7 \pm 0.3) \times 10^{-4}$¶	3.0×10^{-2}	9.0×10^{-3}
		45	L	0.837§§	$(7.5 \pm 0.6) \times 10^{-4}$¶	3.8×10^{-2}	2.0×10^{-2}
		50	L	0.812§§	$(1.1 \pm 0.1) \times 10^{-3}$¶	4.7×10^{-2}	2.3×10^{-2}
		55	L	0.779§§	$(3.7 \pm 0.6) \times 10^{-3}$¶	6.0×10^{-2}	6.2×10^{-2}
		60	L	0.748§§	$(5.1 \pm 0.6) \times 10^{-3}$¶	7.5×10^{-2}	6.8×10^{-2}
		65	L	0.723§§	$(7.3 \pm 0.8) \times 10^{-3}$¶	9.2×10^{-2}	7.9×10^{-2}

*Except when noted, normalized surface densities were obtained from DeYoung and Dill (1988).
#Calculated according to Eq. 6.
§Calculated according to Eq. 9.
¶Single determination; ± values are standard deviations estimated by propagation of errors from both the dynamic light-scattering measurement and the NMR linewidth determination.
‖Calculated from the M_1 data by Morrow et al. (1992) and Eq. 8; as the M_1 values were obtained for perdeuterated lipids, which have main transition temperatures approximately 3–4°C lower than those of protiated lipids, a temperature shift of 3° has been assumed.
**Also reported in Xiang and Anderson (1995b).
##Mean ± standard deviation of two determinations.
§§From Huang, et al. (1993).

Phase structure, surface density, and acetic acid permeability versus lipid chain length, cholesterol concentration, and temperature for bilayers used in this study

The chemical compositions of the bilayers utilized in this study and the temperatures employed are listed in Table 1. Based on published phase diagrams (Almeida et al., 1992; Huang et al., 1993; Vist and Davis, 1990), the bilayer systems described in Table 1 encompass a variety of phase structures including the pure-gel states (L_β or $P_{\beta'}$), the disordered liquid-crystalline state (L_α), the cholesterol-rich liquid-ordered state (L_0), and regions of gel–liquid-crystalline phase coexistence. Inasmuch as the regions of coexistence of the liquid-disordered and the liquid-ordered fluid states have not yet been fully agreed on (Huang et al., 1993; Vist and Davis, 1990), each system listed in Table 1 has been described more simply in terms of the presence of either gel state only (G), liquid-crystalline state only (L), or gel–liquid-crystalline phase coexistence (G-L).

The state of the bilayer can also be characterized in terms of the normalized surface density, $\sigma = A_0/A$, where A is the area per PC molecule and A_0 is its area in the crystal. A universal correlation exists between the C—D bond-order parameter (S_{CD}) of acyl chains in a bilayer membrane and the average area per lipid, irrespective of the chemical structure (i.e., headgroup, number of chains per molecule, chain length) of the lipid (Boden et al., 1991). Thus, the normalized surface density can be obtained from the measured order parameter, S_{mol} ($=-2S_{CD}$), in the plateau region (or the maximum quadrupole splitting in ^{2}H-NMR) by a formula derived from lattice theory (DeYoung and Dill, 1988):

$$\sigma = \tfrac{1}{2}(1 + 2S_{mol}), \tag{7}$$

or from the measured mean order parameter, $-2\langle S_{CD}\rangle$, (or the first moment M_1 ($=-\pi e^2qQ/\sqrt{3}h\langle S_{CD}\rangle$) (Davis, 1983) in ^{2}H-NMR) by means of a molecular model of Schindler and Seelig (1975).

$$\sigma = \tfrac{1}{2}(1 - \langle 2S_{CD}\rangle), \tag{8}$$

Equation 8 is useful in determining the surface density near and below the main phase transition in pure PC bilayers.

The normalized surface densities for each system are listed in Table 1. The majority of the values listed for liquid-crystalline bilayers were reported previously by DeYoung and Dill (1988) from measurements obtained with MLVs composed of DLPC, DMPC, and DPPC or their mixtures with cholesterol at different temperatures. We calculated surface densities at or below the gel → liquid-crystalline phase transition temperature in pure DMPC and DPPC bilayers from the M_1 data of Morrow et al. (1992), using Eq. 8. The results of Huang et al. (1993) were used to calculate the surface densities in all DSPC:cholesterol bilayers and some DPPC:cholesterol bilayers. Huang et al. determined the quadrupole splittings for ^{2}H-containing chains labeled at position 6 (sn-2) in DPPC:cholesterol bilayers and at position 12 (sn-2) in DSPC:cholesterol bilayers over a wide range of cholesterol concentrations and temperatures. The surface densities calculated from these data are in general agreement (<5% error) with the results of DeYoung and Dill (1988) for perdeuterated DPPC bilayers and are 5–10% smaller than those obtained by Hubner and Blume (1987) at 55°C and 60°C for DSPC bilayers ^{2}H-labeled at the 4,4 position. All the DSPC:cholesterol bilayers studied here have higher-order parameters than those examined by Hubner and Blume, and, as a result, the plateau region is expected to expand further into the bilayer interior (Lafleur et al., 1990). Therefore, the error in using the quadrupole splittings for ^{2}H labeled at position 12 (sn-2) in DSPC:cholesterol bilayers to calculate the surface density should be relatively small. Whenever a surface density at a particular temperature was not available, an interpolated value was used. The possibility that order parameters, and consequently surface densities, in LUVs may differ from

those in MLVs because of variation in vesicle size was recently examined by Fenske and Cullis (1993). They found that the order-parameter profiles in POPC-d_{31} LUVs were very similar to those of MLVs with the same temperature and chemical composition, indicating that orientational order in both MLVs and LUVs with diameters $\geq$ 100 nm is essentially the same. Because the LUVs employed in the present study had hydrodynamic diameters between 120 and 220 nm, the assumption is made that bilayer order does not depend on vesicle size.

The variation of the methyl proton linewidth for acetic acid entrapped within DPPC:cholesterol LUVs ($X_{chol} = 0.4$) at pD 5.98 as a function of temperature between 15°C and 48°C is illustrated in Fig. 1. The internal lifetimes, τ_i, obtained from the linewidth measurements were combined with the measured vesicle hydrodynamic diameters d according to Eqs. 2–5 to yield the permeability coefficients P_m listed in Table 1. A survey of these P_m values reveals a variation in permeability coefficients of more than 3 orders of magnitude, depending on lipid chain length, cholesterol content, and temperature. Greater than 2-orders-of-magnitude variability is demonstrated between liquid-crystalline state bilayers, whereas the pure-gel state bilayers in Table 1 exhibit a variability of >40-fold. In the discussions that follow, we consider first the permeability of acetic acid in liquid-crystalline bilayer membranes, after which the effects of phase transitions are examined.

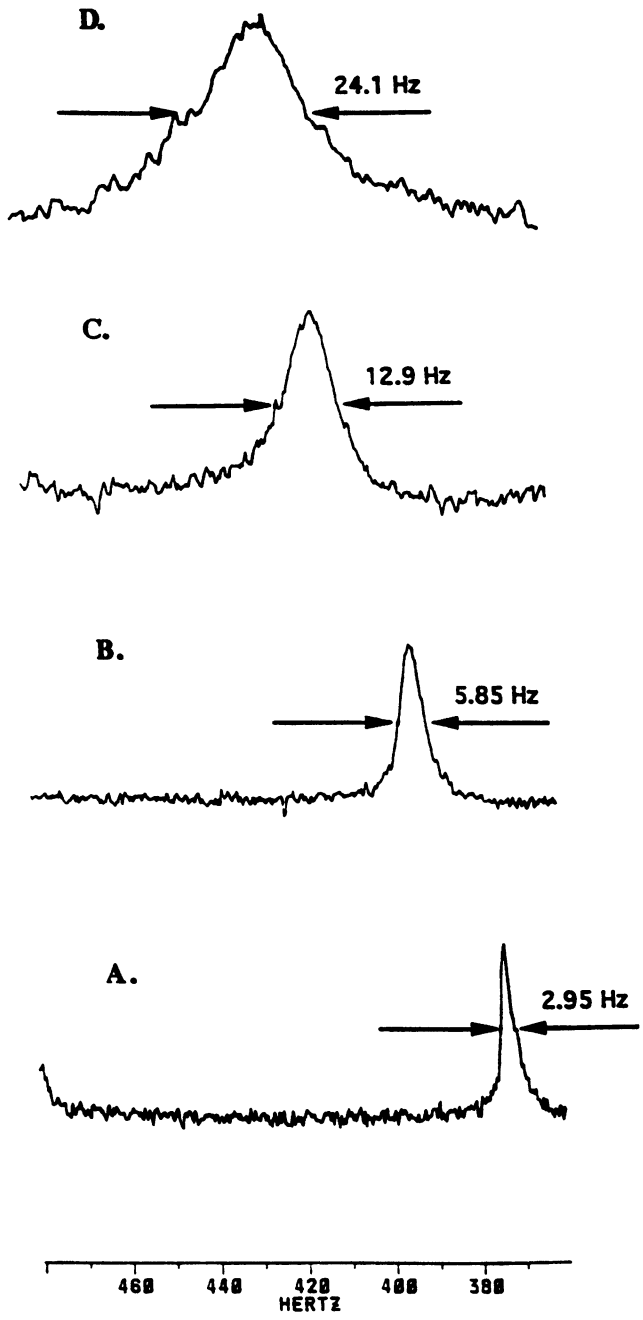

FIGURE 1 NMR signals for the methyl protons of entrapped acetic acid in DPPC:cholesterol LUVs ($X_{chol} = 0.4$) at pD = 5.98 versus temperature: *A*, 15°C; *B*, 30°C; *C*, 40°C; *D*, 48°C. The sweep width was 2.8 kHz, and the pulse width was 4.0 μs. Linewidths at one-half maximum peak height are shown.

Permeability in liquid-crystalline bilayers: the role of surface density

According to solubility-diffusion theory, the permeability coefficient is directly proportional to the product of the partition coefficient and the diffusion coefficient of the permeant in a bulk liquid hydrocarbon or oil divided by the thickness of the hydrocarbon region (Finkelstein, 1976), as described by Eq. 6. P_0 values calculated from Eq. 6 are displayed in Table 1 for the various bilayers examined. These estimates were obtained by use of acetic acid's decane–water partition coefficient and its diffusion coefficient in decane, both of which have been determined as a function of temperature (Xiang and Anderson, 1995b). The bilayer hydrocarbon thickness δ_{hc} was estimated from $l_0\sigma$ (cf. Eq. 4). It is evident that the dramatic variation of >2 orders of magnitude in the permeability coefficients of acetic acid (Table 1) within the liquid-crystalline region with changes in lipid chain length, cholesterol composition, and temperature cannot be rationalized by this model. P_0 values predicted are substantially larger than the observed permeability coefficients and vary by only ≈6-fold over this region. Therefore, the effects of chain ordering are substantial.

Previously, DeYoung and Dill (1988, 1990) suggested that the relevant physical variable to account for bilayer–water partition coefficients of nonpolar solutes is the surface density and not the cholesterol concentration, the temperature, or the phospholipid chain length. We previously extended this treatment to account for the variation in the bilayer–water partition coefficient of acetic acid in DMPC:cholesterol bilayers that vary in cholesterol composition and temperature and demonstrated a steeper, linear dependence between the logarithm of acetic acid's permeability coefficient and the normalized surface density in the same systems (Xiang and Anderson, 1995b).

A similar treatment is considered here in Fig. 2, which shows the natural logarithms of the permeability coeffi-

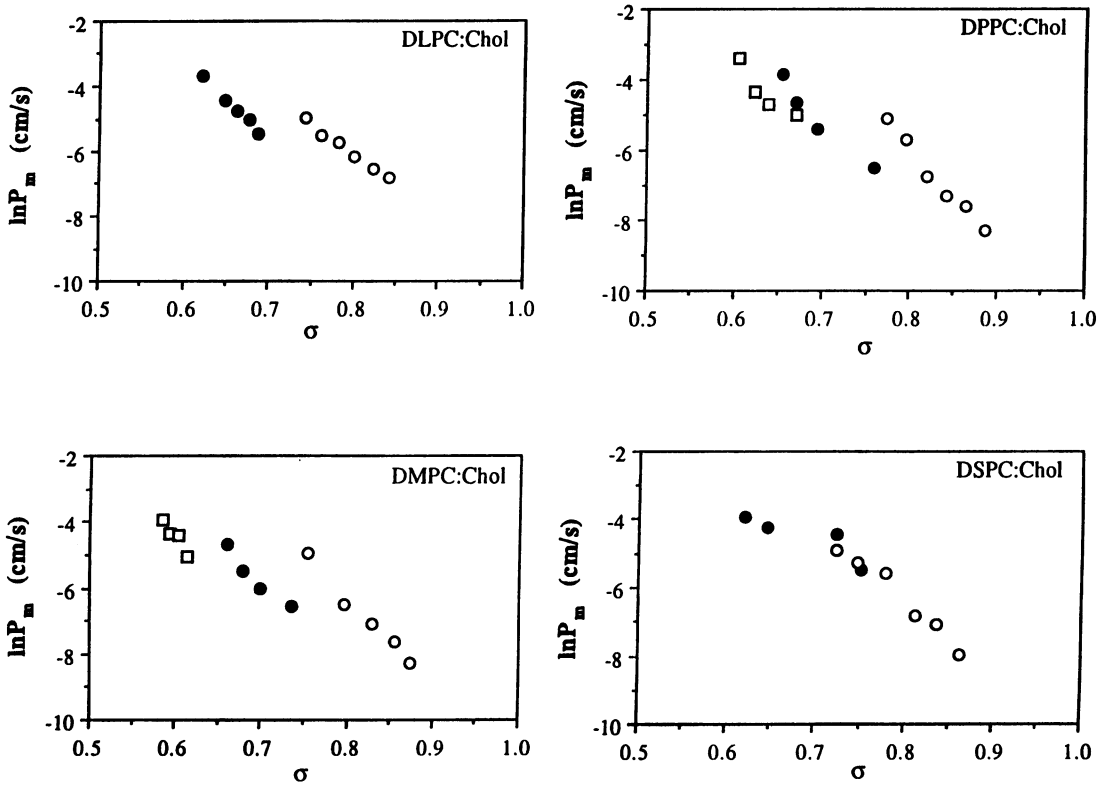

FIGURE 2 Natural logarithms of the permeability coefficients for acetic acid across liquid-crystalline phospholipid:cholesterol bilayers versus the normalized surface density σ: [□], X_{chol} = 0.0; ●, X_{chol} = 0.2; ○, X_{chol} = 0.4.

cients for acetic acid across liquid-crystalline DLPC:cholesterol, DMPC:cholesterol, DPPC:cholesterol, and DSPC:cholesterol bilayers versus the normalized surface density σ. A general trend of decreasing permeability with increasing surface density is evident, suggesting that, indeed, chain-ordering effects play a primary role. The deviations from linearity, which appear to be systematic rather than random, can be accounted for by solubility-diffusion theory. For example:

1) At a given surface density, except in DSPC:cholesterol bilayers, the permeability coefficient at a higher mole fraction of cholesterol exceeded that at a lower mole fraction of cholesterol. Because at a constant surface density the lipid bilayer with a higher cholesterol concentration is generally at a higher temperature, the permeability coefficient should be corrected for those temperature effects that are independent of chain ordering in the lipid bilayers. Such effects include temperature effects on partitioning (e.g., dehydration of the permeant), on the activation energy for "bulk" diffusion, and on thickness of the hydrocarbon region.

2) At a given surface density, the permeability coefficient for acetic acid across a short-chain lipid bilayer generally exceeds that across a long-chain lipid bilayer. This is especially notable in DLPC bilayers. This observation can be rationalized by solubility-diffusion theory, because the permeability coefficient is inversely proportional to the bilayer thickness.

It is now clear that values of ln P_m obtained for acetic acid under a variety of conditions (e.g., various lipid compositions, lipid chain lengths, and temperatures) are determined by the effects of chain ordering superimposed upon the predictions of solubility-diffusion theory. We previously suggested that a more suitable model for lipid bilayer permeabilities is the barrier domain model shown in Eq. 9 (Xiang and Anderson, 1995b). If permeation is rate limited by the ordered hydrocarbon domain within the bilayer, the permeability coefficient P_m can be written as

$$P_m = \frac{K_{barrier/water} D_{barrier}}{\delta_{barrier}} = fP_0, \quad (9)$$

where $K_{barrier/water}$ and $D_{barrier}$ are the partition coefficients from water into and diffusion coefficient in the barrier domain, respectively, and $\delta_{barrier}$ is the barrier thickness. Although the form of Eq. 9 coincides with that of solubility-diffusion theory (Eq. 6), the individual parameters have different meanings, as their values include chain-ordering effects. Thus, P_m equals the product of P_0 from solubility-diffusion theory calculated from Eq. 6 and a scaling factor f, the permeability decrement that is due to chain ordering. In a membrane of randomly oriented chains (i.e., a bulk solvent), f would have a value of 1. Inasmuch as all bilayers exhibit order parameters higher than that which would be exhibited by a system composed of randomly oriented

chains, $f < 1$ for all bilayer systems. Values of f determined from the ratios of P_m/P_0 are listed in Table 1. As expected, f values are substantially less than 1, and changes in f account for most of the variability in P_m.

As demonstrated in Fig. 3, a substantial improvement is obtained in the correlation of $\ln f$ versus σ compared with the $\ln P_m$ versus σ plots (Fig. 2). Especially improved are the results in DLPC:cholesterol and DMPC:cholesterol bilayers, whereas the change is less dramatic for the long-chain lipid bilayers. When all f values obtained at different chain lengths, cholesterol concentrations, and temperature are combined, as shown in Fig. 4, a clear linear relationship ($r = 0.94$) emerges:

$$\ln f = \xi + \kappa\sigma, \tag{10}$$

with a slope of $\kappa = -10.6$ (± 0.6 SE) and intercept of $\xi = 5.3$ (± 0.4 SE). Of the overall $\ln P_m$ range of 4.6 within liquid-crystalline bilayers, chain-ordering effects therefore account for a variation of 3.3 in $\ln P_m$.

In the limit of random orientation of lipid molecules in a bilayer, the order parameter S_{mol} approaches zero, corresponding to a normalized surface density σ of 0.333 (cf. Eq. 7). This hypothetical reference state represents the bulk hydrocarbon solvent-filled membrane of solubility-diffusion theory, and, at this value of σ, f should equal 1. As shown in Fig. 4, however, $\ln f$ passes through 0 ($f = 1$) at $\sigma \approx 0.5$, and extrapolation to $\sigma = 0.333$ yields $f = 5.8$. Several factors may contribute to a deviation of this value from unity. For example, the discrepancy may reflect a less-than-optimal choice of model bulk solvent in calculating P_0, leading to its underestimation and therefore to a positive deviation in f. Studies published previously by the present authors indicated that the barrier domain in egg PC bilayers is more polar/polarizable than decane, resembling more closely the microenvironment in decadiene (Xiang and Anderson, 1994b; Xiang and Anderson, 1994c; Xiang

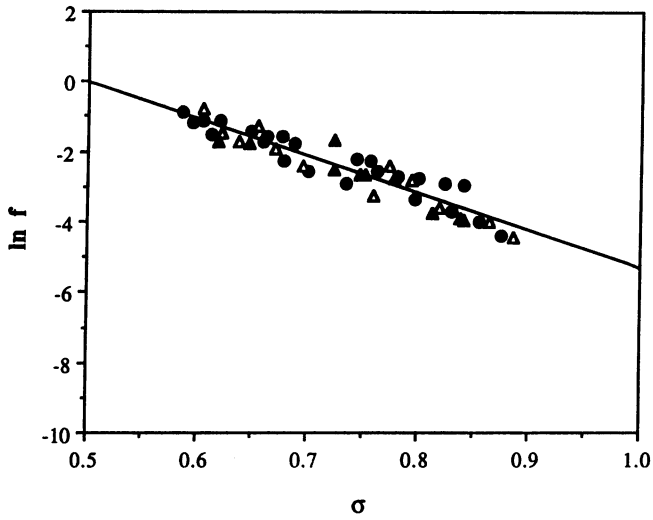

FIGURE 4 Combined data from the four panels in Fig. 3. The solid curve is a least-squares fit of all the data: ●, DLPC:cholesterol; ○, DMPC:cholesterol; △, DPPC:cholesterol; ▲, DSPC:cholesterol.

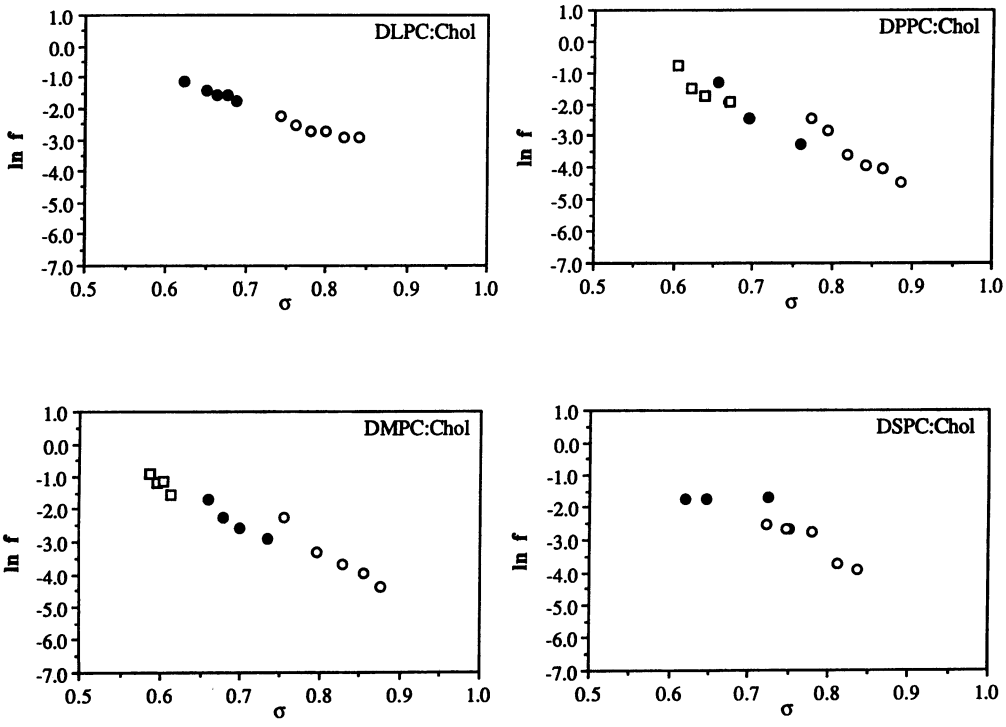

FIGURE 3 Natural logarithms of f (Eq. 9) for acetic acid across liquid-crystalline phospholipid:cholesterol bilayers versus the normalized surface density σ: □, $X_{chol} = 0.0$; ●, $X_{chol} = 0.2$; ○, $X_{chol} = 0.4$.

et al., 1992). Acetic acid has a decadiene–water partition coefficient 4.2-fold larger than that between decane and water (Xiang and Anderson, 1994b). Thus, the discrepancy may be attributable to a more favorable partitioning of acetic acid into the barrier domain than suggested by its decane–water partition coefficient. Decane was chosen as the model bulk solvent because, unlike those in egg PC, the lipid chains in the PC bilayers employed in this study were fully saturated, and the temperature dependence of acetic acid's partition coefficient and diffusion coefficient were known. A more suitable model solvent may ultimately be found, leading to an improvement in the estimate of f at $\sigma = 0.333$, but the choice of model bulk solvent would not be expected to alter significantly the slope of the plot in Fig. 4, which is the main focus of this study.

The temperature dependencies of the permeability coefficients for acetic acid across DLPC:cholesterol, DMPC:cholesterol, DPPC:cholesterol, and DSPC:cholesterol liquid-crystalline bilayers at several cholesterol concentrations are shown in Fig. 5. At $X_{chol} = 0.2$ and below the main phase transitions, DPPC and DSPC bilayers are in the gel–liquid-crystalline phase coexistence region. As a result, two distinct permeation routes through the gel and the liquid-crystalline domains (P_g and P_{lc}) must be considered, and the overall permeability coefficient can be expressed as

$$P_m = (1 - f_{lc})P_g + f_{lc}P_{lc}, \quad (11)$$

where f_{lc} is the fraction of the liquid-crystalline domain. Because P_g is generally much smaller than P_{lc}, the observed P_m values in the gel–liquid-crystalline coexistence regions were divided by f_{lc} to yield estimates of P_{lc}, which were then plotted along with other permeability data in liquid-crystalline phases in Fig. 5. Least-squares fits of these Arrhenius plots produced the apparent activation energies (E_a) for the permeation of acetic acid as a function of chain length and cholesterol concentration shown in Table 2. At a given cholesterol composition the apparent activation energy for permeation of acetic acid across the lipid bilayers increases with phospholipid chain length. Activation energies within a similar range have been reported for the transport of *n*-alkylamines across egg–lecithin bilayers (≈20 kcal/mol; Bar-On and Degani, 1985), for glucose from DMPC/DCP vesicles (26 kcal/mol; Bresseleers et al., 1984), and for polyhydroxyalcohols through DMPC/30% cholesterol membranes (14–25 kcal/mol; de Gier et al., 1971). Subczynski et al. (1990) reported that the translational diffusion of a copper complex, $CuKTM_2$, in DMPC:cholesterol bilayers ($X_{chol} = 0.0, 0.3$) has an activation energy in the 9–18-kcal/mol range.

These relatively high apparent activation energies and their dependence on chain length are difficult to explain on the basis of either the solubility-diffusion model or a transient aqueous pore model. Transient pore formation was

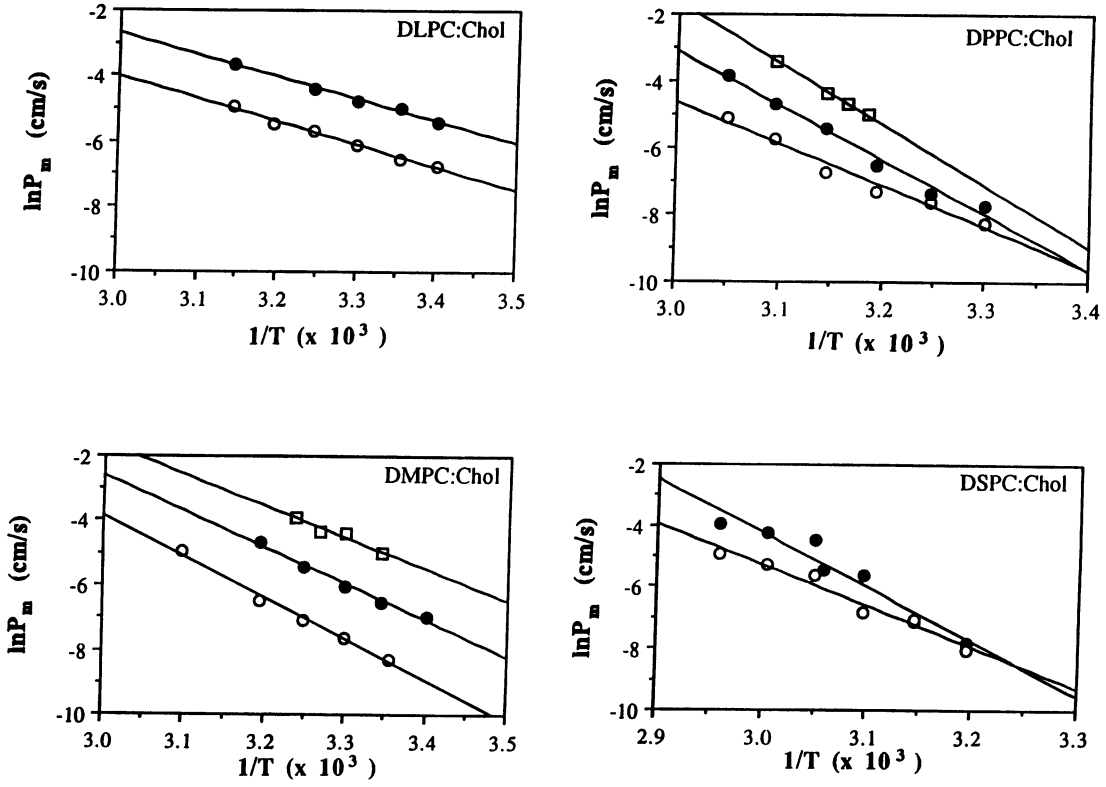

FIGURE 5 Arrhenius plots of the permeability coefficients for acetic acid across liquid-crystalline phospholipid:cholesterol bilayers at different mole fractions of cholesterol: □, $X_{chol} = 0.0$; ●, $X_{chol} = 0.2$; ○, $X_{chol} = 0.4$.

TABLE 2 Apparent activation energies for permeation calculated from the temperature dependence of the permeability coefficients for acetic acid across saturated PC: cholesterol lipid bilayers

	E_a (kcal/mol)			
X_{chol}	DLPC	DMPC	DPPC	DSPC
0.00	–	20 ± 3	37 ± 1	–
0.20	13 ± 1	22 ± 2	33 ± 2	35 ± 4
0.40	14 ± 1	25 ± 2	25 ± 2	27 ± 2

Energies are expressed as fitted values ± standard deviation.

recently suggested to account for the permeation of water molecules across lipid bilayers, as low activation energies (2–8 kcal/mol), similar to that for self-diffusion of bulk water, have been observed for water permeation (Jansen and Blume, 1995). In the solubility-diffusion model it is the dehydration energy that is usually considered to be the dominant component of the activation energy for solute transport (Bindslev and Wright, 1976; Bresseleers et al., 1984; de Gier et al., 1971; Stein, 1986). E_a^{bulk} (=8.0 kcal/mol) estimated from the solubility-diffusion model (from the temperature dependence of acetic acid's decane–water partition coefficient and diffusion coefficient in decane) and the activation energies for water permeation are much smaller than the E_a values observed for permeation of acetic acid across bilayers composed of DMPC, DPPC, DSPC, and their mixtures with cholesterol. Thus, for these lipid bilayers, at least those with chain lengths greater than 12 carbons, neither the classical solubility-diffusion model nor transient pore formation can account for more than a minor fraction of the overall activation energy. E_a^{bulk} estimated from the solubility-diffusion model is closer to the E_a values obtained in short-chain bilayers (e.g., DLPC:cholesterol) in which acyl chains are generally more disordered and impose a weaker resistance to the permeation of acetic acid.

The contribution of chain ordering within lipid bilayers may account for the additional permeability barrier relative to that estimated from solubility-diffusion theory, as those bilayers that are more ordered, as judged by their surface densities, yield the lowest permeability coefficients. Similarly, the added contribution to the activation energy that is due to the variation of chain order with temperature may account for the large apparent activation energies observed. Chain ordering may affect permeant diffusion coefficients through alterations in medium viscosity or membrane "fluidity" (de Gier, 1993; Lande et al., 1995; Lieb and Stein, 1971; Pace and Chan, 1982) or permeant partition coefficients by expulsion of solute (DeYoung and Dill, 1988, 1990; Xiang and Anderson, 1994a). Both effects are probably involved.

Assuming that E_a^{bulk} reflects the temperature dependence of acetic acid's decane–water partition coefficient and the diffusion coefficient in decane and correcting for the dependence of bilayer thickness on σ (Eq. 4), we can combine Eqs. 9 and 10 to obtain the following relationship for the membrane permeability coefficient:

$$\ln P_m(T) = C + \frac{-E_a^{bulk}}{RT} - \ln \sigma + \kappa\sigma, \qquad (12)$$

where C and κ are constants that are independent of temperature, R is the gas constant, and $\sigma = A_0/A$ is the normalized surface density. The apparent activation energy, E_a, can then be written as

$$E_a = E_a^{bulk} + R(\kappa - 1/\sigma)\frac{\partial\sigma}{\partial(1/T)}. \qquad (13)$$

As $|\kappa|$ (=10.6) $\gg 1/\sigma$, the dependence of E_a on $\partial\sigma/\partial(1/T)$ is expected to be approximately linear. Fig. 6 shows the apparent activation energy E_a relative to $\partial\sigma/\partial(1/T)$. A linear least-squares fit gave a slope of 25.1 ± 5.6 kcal/mol/deg and an intercept of 10.9 ± 3.5 kcal/mol, with r = 0.85. Within the uncertainty limits, the intercept, or E_a^{bulk}, is close to that (8.0 kcal/mol) estimated from separate bulk partitioning and diffusion experiments (Xiang and Anderson, 1995b). These results suggest that the contributions that are due to chain ordering within the bilayer membrane and to the variation of chain packing with temperature are primarily responsible for the large apparent activation energies.

Effects of phase and phase transitions in DMPC and DPPC bilayers on permeability

As shown in Table 1, in pure DMPC and DPPC bilayers acetic acid permeability coefficients were generated over a temperature range that included both gel-state and liquid-crystalline bilayers. The effects of the phase and phase transitions on the permeability of acetic acid across DPPC and DMPC bilayers (X_{chol} = 0.0) are illustrated in Fig. 7. Permeability across gel-phase DSPC bilayers could not be detected by the present method. Permeability coefficients

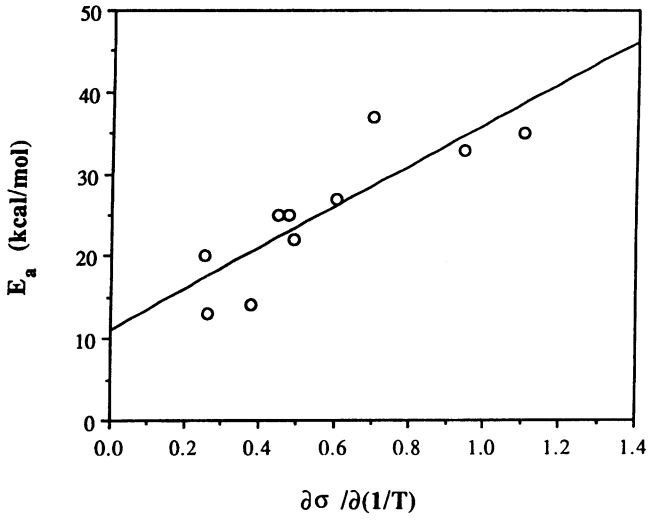

FIGURE 6 Apparent activation energy E_a for the permeability of acetic acid as obtained from the Arrhenius plots in Fig. 5 versus $\partial\sigma/\partial(1/T)$.

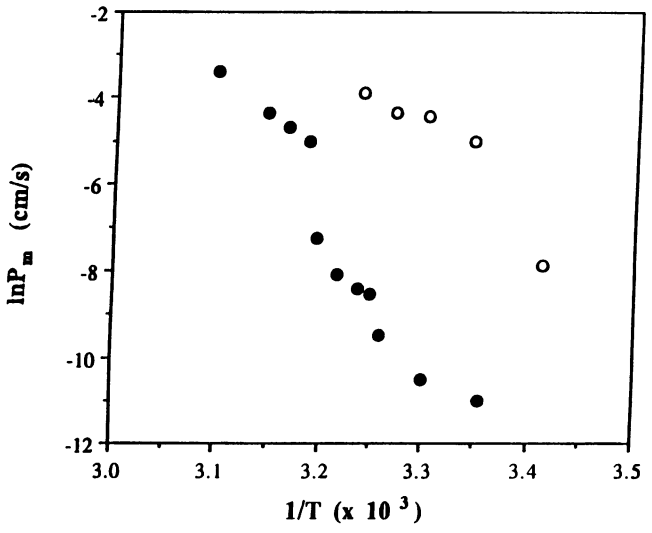

FIGURE 7 Arrhenius plots of the permeability coefficients for acetic acid across gel and liquid-crystalline DMPC (○) and DPPC (●) bilayers (X_{chol} = 0.0).

across pure gel and liquid-crystalline DLPC bilayers could also not be determined because, we speculate, of the fast fusion of the DLPC LUVs in the presence of the chemical shift reagent, Pr^{+3}.

The permeability coefficient of acetic acid at a temperature 4°C above the main transition temperature (T_m) in DPPC bilayers (=(1.3 ± 0.1) × 10^{-2} cm/s), was found to be 59-fold larger than P_m (=(2.2 ± 0.6) × 10^{-4} cm/s) 5°C below the T_m of 41°C and 482-fold larger than P_m (=(2.4 ± 0.6) × 10^{-5} cm/s) 5°C below the pretransition temperature (35°C). Two sharp declines in the permeability coefficient versus temperature profiles are clearly seen at the pretransition and the main transition. (The abrupt change of the permeability coefficient in DPPC bilayers at 41 ± 1°C indicates that the transition temperature for the DPPC bilayers studied was not greatly changed in the presence of 1–5 mM Pr^{+3}, in contrast to previous studies in DPPC bilayers at higher Pr^{+3} concentrations (i.e., 10 mM), in which changes in the phase transition temperature of 2–3°C were observed (Negrete et al., 1996).) A similar decline in permeability coefficient was also observed near T_m in DMPC bilayers, in which the permeability coefficient 6°C above T_m, P_m = (1.2 ± 0.4) × 10^{-2} cm/s, was 31-fold larger than P_m (=(3.9 ± 0.5) × 10^{-4} cm/s) 4°C below T_m = 24°C. A recent study of water permeability across diacyl PC bilayers by a vesicle swelling method found a permeability reduction of ≈100-fold when temperature was lowered through the main phase transition (Jansen and Blume, 1995). A study of diffusion of small nitroxide solutes in DPPC liposomes by ^{13}C spin relaxation spectroscopy similarly demonstrated that the viscosity in the bilayer interior increases sharply by >100-fold when the temperature is lowered below T_m (Dix et al., 1978).

Unified treatment of permeabilities in both gel and liquid-crystalline phases: dependence on free-surface area per lipid molecule

We have shown that in liquid-crystalline bilayers the permeability coefficient predicted from solubility-diffusion theory must be adjusted downward by a factor f, which accounts for the effects of lipid chain ordering on permeability. The natural logarithm of this factor was shown to depend linearly on bilayer surface density. To examine whether such a relationship remains linear at and below the main phase transition, one needs to know the relevant surface densities, preferentially from ^2H-NMR measurements for consistency. Although there is no strong theoretical reason for correlating the measured first moment in ^2H-NMR with the surface density below the main transition, as noted by Morrow et al. (1992), neutron and x-ray-diffraction measurements of the surface area for DPPC bilayers at 20°C agree very closely (<3% error) with ^2H-NMR measurements using Eq. 8, which are valid for liquid-crystalline phases. Thus, following a practice adopted in several other studies (Davis, 1979; Vist and Davis, 1990), we have employed Eq. 8 to calculate the normalized surface density σ from known M_1 data below the main phase transitions in DMPC and DPPC bilayers.

Shown in Fig. 8A are the natural logarithms of the permeability decrement (f) for acetic acid across pure DMPC and DPPC bilayers near their respective main transitions as a function of the surface density, σ. The solid curve is the same as that shown in Fig. 4. Although the data above the main transitions follow the regression line closely, the permeability data generated below the transition temperatures exhibit progressively larger deviations as temperature is lowered and the tilted gel phase ($L_{\beta'}$) is reached. At a temperature of 25°C, approximately 9°C below the pretransition in DPPC bilayers, the value of f is 13.6 times smaller than the one predicted by extrapolation of the ln f versus σ relationship established for the liquid-crystalline bilayers to the value of σ (=0.892) at that temperature.

A large body of evidence indicates that in the gel phase the lipid chains are predominantly in an all-*trans* conformation and collectively tilted from the bilayer normal (Cameron et al., 1981; Davis, 1979). The steep decrease in P_m with temperature in the gel phase may originate from a change in the molecular packing of the acyl chains from near hexagonal to orthorhombic or monoclinic (Cameron et al., 1980). In a previous theoretical work (Xiang and Anderson, 1994a) we showed that the reversible volume work needed for the creation of free volume for the partitioning of a permeant into the bilayer interior is proportional to the local lateral pressure within the bilayer. The relationship between surface tension (π) and surface density in lipid monolayers and bilayers deviates only slightly from linearity in the range σ = 0.50–0.85, but π varies more steeply as the lipid area approaches that in a gel phase (Mingins et al., 1982; Wolfe and Brockman, 1988). For a qualitative comparison with the permeability data, a π–σ relation ob-

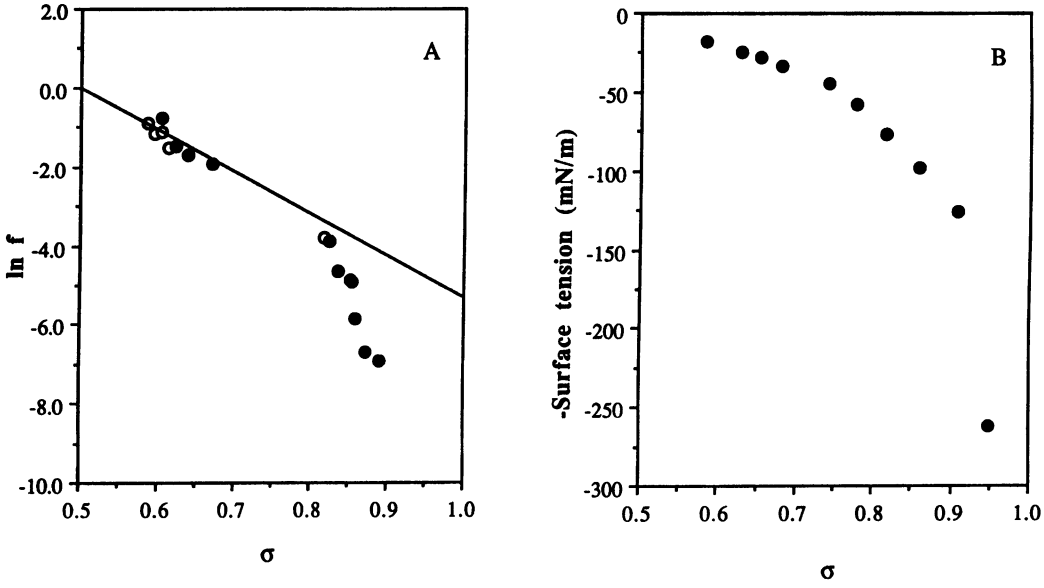

FIGURE 8 *A*, Natural logarithms of f for acetic acid across gel and liquid-crystalline DMPC (○) and DPPC (●) bilayers (X_{chol} = 0.0) versus surface density σ. The solid curve is the best fit to the data in Fig. 4. *B*, A π–σ relation obtained in POPC monolayers and egg PC bilayers by Wolfe and Brockman (1988).

tained in POPC monolayers and egg PC bilayers (Wolfe and Brockman, 1988) is plotted in Fig. 8 *B*. The ln f versus σ profile bears a qualitative resemblance to that for π versus σ.

Molecular diffusion in simple liquids and polymers and lipid lateral diffusion in bilayer membranes have been successfully described by free-volume theory (Hildebrand, 1977; Vaz et al., 1985; Vrentas, 1977). In the original Cohen–Turnbull diffusion theory (Cohen and Bangham, 1972; Turnbull and Cohen, 1970), translational diffusion of a molecule is assumed to occur when statistical redistribution of free volume opens up a cavity of a critical size in the immediate vicinity of the molecule. As a result, the diffusion coefficient is proportional to the probability of finding a free volume with a certain size, V^*, which is usually formulated as an exponential function (for a more detailed discussion of free-volume distributions in lipid bilayers, see Xiang (1993)). The three-dimensional model of Cohen and Turnbull has been used to describe the effects of permeant size on transport across biological membranes (Stein, 1986). Others have modified the Cohen–Turnbull theory (Galla et al., 1979; Vaz et al., 1985) to describe the lateral diffusion of lipophilic probes in bilayer membranes in terms of the average free area, rather than free volume, per lipid molecule. Similar to the definition of free volume (Bondi, 1954), the average free area per lipid molecule, a_f, can be expressed as

$$a_f = A - A_0 = A_0(1/\sigma - 1), \tag{14}$$

where A is the area per lipid molecule, A_0 is its area in the crystal, and σ is the normalized surface density (cf. Eq. 4).

We propose that a free-surface-area model may also be applicable to *trans*-bilayer permeability, as *trans*-bilayer permeability depends on the two-dimensional packing structure of lipids, which can be characterized by the free surface area per lipid molecule, a_f. Both the barrier domain–water partition coefficient $K_{barrier/water}$ and the diffusion coefficient within the barrier domain $D_{barrier}$ may be functions of a_f. By analogy with Cohen–Turnbull theory, the dependence of the diffusion coefficient on a_f can be given by

$$D_{barrier} = D_0 \exp(-\gamma a^*/a_f), \tag{15}$$

where a^* can be considered the effective cross-sectional area of the permeating solute and γ is a constant. In free-volume theory, γ is assumed to have a value between 1/2 and 1 to account for any overlapping free volumes (Cohen and Turnbull, 1959). D_0 combines all other known and unknown factors such as a geometrical factor and the average velocity of the permeant (Galla et al., 1979).

The chemical potential of a solute in a lipid bilayer is the ensemble average of $\exp(-U/k_BT)$, where U is the overall interaction energy between the solute and the surrounding lipid molecules and k_B is Boltzmann's constant. Among various molecular interactions, the short-range repulsive interaction plays a primary role (Meraldi and Schlitter, 1981; Warner, 1980). Thus, the number of accessible states for solute partitioning into the bilayer interior is also determined by the free-volume distribution. The steric partitioning behavior of molecules into porous networks and membranes has been described by a free-volume statistical physics model (Schnitzer, 1988), a simple extension of which leads to the following expression for the partition coefficient into a bilayer membrane:

$$K_{barrier/water} = K_0 \exp(-a^*/a_f). \tag{16}$$

More recently, the present authors have explored the effects of the volume expansion required for cavity formation on solute distributions in interphases (Xiang and Anderson, 1994a). The excluded-volume partition coefficient can be written as

$$K_{\text{barrier/water}} = K_0 \exp(-2(p_\perp - 1)V^*/3k_BT), \quad (17)$$

where $p_\perp$ is the lateral pressure and V^* is the permeant volume. The surface-tension data in Fig. 8 *B* are linearly correlated with $1/a_f$ ($r = 0.995$), suggesting that our statistical mechanics model and the one developed by Schnitzer (1988) have similar functional dependencies on membrane packing properties.

Combining Eqs. 14–16, we obtain the following expression for the dependence of f on free-surface area:

$$\ln f = \ln f_0 - \frac{(\gamma + 1)a^*}{a_f} = \ln f_0 - \frac{(\gamma + 1)a^*}{A_0} \frac{\sigma}{(1 - \sigma)}, \quad (18)$$

where f_0 is the permeability decrement for a hypothetical point solute. Fig. 9 displays the combined data for the natural logarithms of f obtained from the permeability coefficients of acetic acid across both gel and liquid-crystalline bilayers relative to $A_0/a_f = \sigma/(1 - \sigma)$. An excellent linear correlation ($r = 0.93$) results with $\ln f = -0.305 - 0.713\ A_0/a_f$. Remarkably, the permeability of acetic acid across both liquid-crystalline and gel phases can be described by the same fundamental molecular packing property of the lipid bilayers, namely, the underlying free-surface-area distribution. However, the functional form of Eq. 18 between f and free-surface area may not be exclusive, as other analytical functions may also give satisfactory correlations (e.g., a power law dependence of the diffusion coefficient on the mean free volume in polymers was recently proposed by Mauritz et al. (1990)).

Acetic acid has a van der Waals volume of 55.5 Å^3 (Xiang and Anderson, 1994b). Thus, a spherical approximation would give a cross-sectional area of $a^* = 17.6$ Å^2 for acetic acid. The true a^* may be slightly smaller, as the permeant is not strictly spherical and may align itself partially in the bilayer interior with its long principal axis along the bilayer normal. As phospholipid molecules have an area of 40.8 Å^2 in their crystalline states, the slope of the regression line in Fig. 9 using Eq. 18 yields $(\gamma + 1)a^* = 29.1$ Å^2, corresponding to an estimated γ of 0.65, within the range of values assumed in the free-volume theory of Cohen and Turnbull (1959).

CONCLUDING REMARKS

The barrier to solute transport across lipid bilayer membranes, when it is considered in terms of an "activation" free energy as illustrated schematically in Fig. 10, consists of several components. Those typically considered in solubility-diffusion theory are the thickness of the bilayer and the permeant's bulk solvent–water partition coefficient and diffusion coefficient in a bulk model solvent chosen to represent the chemical nature of the hydrocarbon region of the bilayer. Solubility-diffusion theory neglects the contributions of the chain order of phospholipid molecules in the bilayers and the phases and phase transitions, which can be considered approximately in terms of their effects on chain order or on other bilayer properties (e.g., surface density–lateral pressure).

Fig. 10 suggests that in some instances chain-ordering effects may predominate. This conclusion is based on the following observations from this study:

1) Within liquid-crystalline bilayers, chain-ordering effects accounted for a variation of 3.3 in ln P_m out of an overall ln P_m range of 4.6. In gel-state and liquid-crystalline

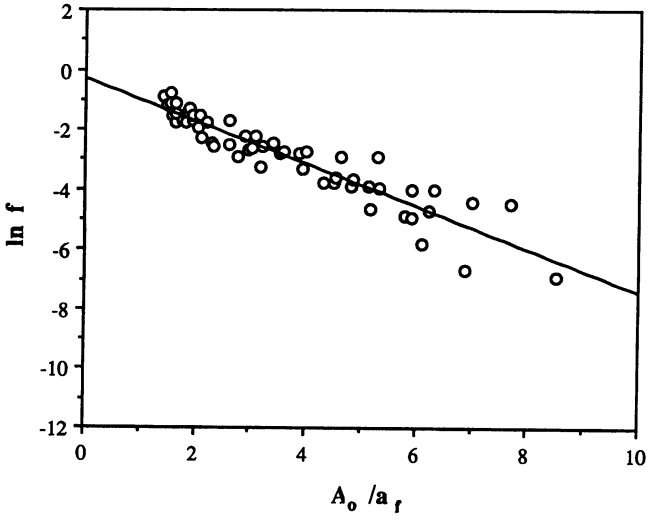

FIGURE 9 Natural logarithms of f for acetic acid across both gel and liquid-crystalline phospholipid:cholesterol bilayers versus the normalized free area, $A_0/a_f = \sigma/(1 - \sigma)$.

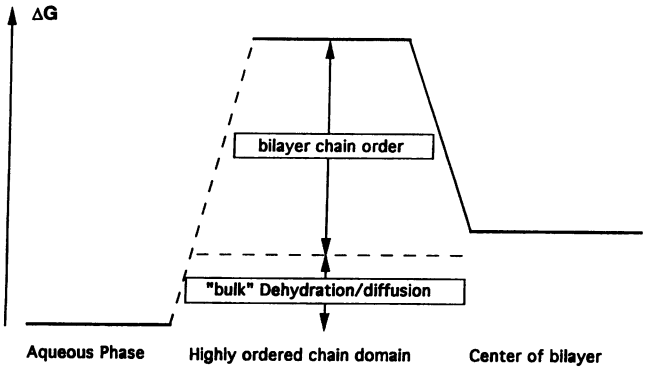

FIGURE 10 Schematic illustration of the components of the free energy of activation for transport of acetic acid across lipid bilayer membranes. The "bulk" contributions (e.g., dehydration, diffusion) refer to those components of the barrier predicted from solubility-diffusion theory, which treats the lipid bilayer as a bulk lipid solvent. Chain-ordering effects are the predominant factor that governs the transport of acetic acid with changes in lipid composition, chain length, or temperature.

bilayers combined, chain-ordering effects accounted for a variation of 6.1 in ln P_m out of an overall ln P_m range of 7.6.

2) The overall activation energies obtained from acetic acid permeability coefficients in fully or partially liquid-crystalline bilayers were found to be substantially greater (Table 2) than the energy of activation estimated from considerations of the temperature dependence of the "bulk" solvent–water (i.e., decane–water) partition coefficient and the diffusion coefficient of acetic acid in decane. The overall activation energies were shown to depend strongly on the variation of chain order (or surface density) with temperature.

The barrier domain model proposed in this study considers membrane permeability in terms of the value predicted from solubility-diffusion theory corrected for chain-ordering effects through the permeability decrement *f*. This factor appears to be a universal and linear function of the bilayer free-surface area, regardless of whether the free-surface area is varied by changes in temperature, bilayer composition, or phase structure.

These conclusions pertain, however, to a single solute (acetic acid) and a limited range of lipid compositions as employed in this study. Moreover, we have assumed that the chemical nature of the barrier microenvironment does not change significantly with lipid composition or phase structure. These assumptions will be tested in future research.

This research was supported by grants from the National Institutes of Health (GM51347), INTERx/Merck, Inc., and the University of Utah Research Committee.

REFERENCES

Alger, J. R., and J. H. Prestegard. 1979. Nuclear magnetic resonance study of acetic acid permeation of large unilamellar vesicle membranes. *Biophys. J.* 28:1–14.

Almeida, P. F. F., W. L. C. Vaz, and T. E. Thompson. 1992. Lateral diffusion in the liquid phases of dimyristoylphosphatidylcholine/cholesterol lipid bilayers: a free volume analysis. *Biochemistry.* 31: 6739–6747.

Bangham, A. D., M. M. Standish, and J. C. Watkins. 1965. Diffusion of univalent ions across the lamellae of swollen phospholipids. *J. Mol. Biol.* 13:238–252.

Barenholtz, Y. 1984. Sphingomyelin-lecithin balance in membranes: composition, structure, and function relationships. *In* Physiology of Membrane Fluidity. M. Shinitzky, editor. CRC Press, Boca Raton, FL. 131–173.

Bar-On, Z., and H. Degani. 1985. Permeability of alkylamines across phosphatidylcholine vesicles as studied by ^{1}H-NMR. *Biochim. Biophys. Acta.* 813:207–212.

Bindslev, N., and E. M. Wright. 1976. Effect of temperature on nonelectrolyte permeation across the toad urinary bladder. *J. Membr. Biol.* 29:265–288.

Boden, N., S. A. Jones, and F. Sixl. 1991. On the use of deuterium nuclear magnetic resonance as a probe of chain packing in lipid bilayers. *Biochemistry.* 30:2146–2155.

Bondi, A. 1954. Free volumes and free rotation in simple liquids and liquid saturated hydrocarbons. *J. Phys. Chem.* 58:929–939.

Bresseleers, G. J. M., H. L. Goderis, and P. P. Tobback. 1984. Measurement of the glucose permeation rate across phospholipid bilayers using small unilamellar vesicles. Effect of membrane composition and temperature. *Biochim. Biophys. Acta.* 772:374–382.

Cameron, D. G., H. L. Casal, E. F. Gudgin, and H. H. Mantsch. 1980. The gel phase of dipalmitoyl phosphatidylcholine: an infrared characterization of the acyl chain packing. *Biochim. Biophys. Acta.* 596:463–467.

Cameron, D. G., H. L. Casal, H. H. Mantsch, Y. Boulanger, and I. C. P. Smith. 1981. The thermotropic behavior of dipalmitoyl phosphatidylcholine bilayers. A Fourier transform infrared study of specifically labeled lipids. *Biophys. J.* 35:1–15.

Cohen, B. E., and A. D. Bangham. 1972. Diffusion of small non-electrolytes across liposome membranes. *Nature (London).* 236: 173–174.

Cohen, M. H., and D. Turnbull. 1959. Molecular transport in liquids and glasses. *J. Chem. Phys.* 31:1164–1168.

Collander, R. 1954. The permeability of *Nitella* cells to non-electrolytes. *Physiol. Plant.* 7:420.

Collander, R., and H. Barlund. 1933. Permeabilitatsstudien an Chara ceratophylla. *Acta Bot. Fenn.* 11:1–114.

Davis, J. H. 1979. Deuterium magnetic resonance study of the gel and liquid crystalline phases of dipalmitoyl phosphatidylcholine. *Biophys. J.* 27:339–358.

Davis, J. H. 1983. The description of membrane lipid conformation, order and dynamics by ^{2}H-NMR. *Biochim. Biophys. Acta.* 737:117–171.

de Gier, J. 1993. Osmotic behaviour and permeability properties of liposomes. *Chem. Phys. Lipids.* 64:187–196.

de Gier, J., J. G. Mandersloot, J. V. Hupkes, R. N. McElhaney, and W. P. van Beek. 1971. On the mechanism of non-electrolyte permeation through lipid bilayers and through biomembranes. *Biochim. Biophys. Acta.* 233:610–618.

DeYoung, L. R., and K. A. Dill. 1988. Solute partitioning into lipid bilayer membranes. *Biochemistry.* 27:5281–5289.

DeYoung, L. R., and K. A. Dill. 1990. Partitioning of nonpolar solutes into bilayers and amorphous *n*-alkanes. *J. Phys. Chem.* 94:801–809.

Dix, J. A., D. Kivelson, and J. A. Diamond. 1978. Molecular motion of small nonelectrolyte molecules in lecithin bilayers. *J. Membr. Biol.* 40:315–342.

Fenske, D. B., and P. R. Cullis. 1993. Acyl chain orientational order in large unilamellar vesicles: comparison with multilamellar liposomes: a ^{2}H and ^{31}P nuclear magnetic resonance study. *Biophys. J.* 64: 1482–1491.

Finkelstein, A. 1976. Water and nonelectrolyte permeability of lipid bilayer membranes. *J. Gen. Physiol.* 68:127–135.

Finkelstein, A. 1987. Water Movement Through Lipid Bilayers, Pores, and Plasma Membranes: Theory and Reality. Wiley Interscience, New York.

Galla, H.-J., W. Hartmann, U. Theilen, and E. Sackmann. 1979. On two-dimensional passive random walk in lipid bilayers and fluid pathways in biomembranes. *J. Membr. Biol.* 48:215–236.

Hildebrand, J. H. 1977. Viscosity and Diffusivity. John Wiley & Sons, New York.

Huang, T.-H., C. W. B. Lee, S. K. Das Gupta, A. Blume, and R. G. Griffin. 1993. A ^{13}C, and ^{2}H nuclear magnetic resonance study of phosphatidylcholine/cholesterol interactions: characterization of liquid-gel phases. *Biochemistry.* 32:13277–13287.

Hubner, W., and A. Blume. 1987. ^{2}H-NMR spectroscopic investigations of phospholipid bilayers. *Bunsenges. Phys. Chem.* 91:1127–1132.

Jansen, M., and A. Blume. 1995. A comparative study of diffusive and osmotic water permeation across bilayers composed of phospholipids with different headgroups and fatty acyl chains. *Biophys. J.* 68: 997–1008.

Korman, S., and V. K. LaMer. 1936. Deuterium exchange equilibria in solution and the quinhydrone electrode. *J. Am. Chem. Soc.* 58: 1396–1403.

Lafleur, M., P. R. Cullis, and M. Bloom. 1990. Modulation of the orientational order profile of the lipid acyl chain in the L_α phase. *Eur. Biophys. J.* 19:55–62.

Lampe, M. A., M. L. Williams, and P. M. Elias. 1983. Human epidermal lipids: characterization and modulations during differentiation. *J. Lipid Res.* 24:131–140.

Lande, M. B., J. M. Donovan, and M. L. Zeidel. 1995. The relationship between membrane fluidity and permeabilities to water, solutes, ammonia, and protons. *J. Gen. Physiol.* 106:67–84.

Lieb, W. R., and W. D. Stein. 1971. The molecular basis of simple diffusion within biological membranes. *Curr. Top. Membr. Transp.* 11:1–39.

Lieb, W. R., and W. D. Stein. 1986. Simple diffusion across the membrane bilayer. *In* Transport and Diffusion Across Cell Membranes. W. D. Stein, editor. Academic Press, Inc., Orlando, FL. 69–112.

Magin, R. L., and M. R. Niesman. 1984. Temperature dependent permeability of large unilamellar liposomes. *Chem. Phys. Lipids.* 34:245–256.

Marqusee, J. A., and K. A. Dill. 1986. Solute partitioning into chain molecule interphases: monolayers, bilayer membranes, and micelles. *J. Chem. Phys.* 85:434–444.

Mauritz, K. A., R. F. Storey, and S. E. George. 1990. A general free volume based theory for the diffusion of large molecules in amorphous polymer above Tg. 1. Application to di-*n*-alkyl phthalates in PVC. *Macromolecules.* 23:441–450.

Meraldi, J.-P., and J. Schlitter. 1981. A statistical mechanical treatment of fatty acyl chain order in phospholipid bilayers and correlation with experimental data. A. Theory. *Biochim. Biophys. Acta.* 645:183–192.

Mingins, J., J. A. G. Taylor, B. A. Pethica, C. M. Jackson, and B. Y. T. Yue. 1982. Phospholipid monolayers at non-polar oil/water interfaces. Part 3. Effect of chain length on phase transitions in saturated di-acyl lecithins at the *n*-heptane/aqueous sodium chloride interface. *J. Chem. Soc. Faraday Trans. 1* 78:323–339.

Morrow, M. R., J. P. Whitehead, and D. Lu. 1992. Chain-length dependence of lipid bilayer properties near the liquid crystal to gel phase transition. *Biophys. J.* 63:18–27.

Nagle, J. H., and D. A. Wilkinson. 1978. Lecithin bilayers: density measurements and molecular interactions. *Biophys. J.* 23:159–175.

Negrete, H. O., R. L. Rivers, A. H. Gough, M. Colombini, and M. L. Zeidel. 1996. Individual leaflets of a membrane bilayer can independently regulate permeability. *J. Biol. Chem.* 271:11,627–11,1630.

Olson, F., C. A. Hunt, F. C. Szoka, W. J. Vail, and D. Papahadjopoulous. 1979. Preparation of liposomes of defined size distribution by extrusion through polycarbonate membranes. *Biochim. Biophys. Acta.* 557:9–23.

Overton, E. 1896. Ueber die osmotischen Eigenschaften der Zelle in ihrer Bedeutung fur die Toxokologie und Pharmakologie. *Vjschr. Naturforsch. Ges. Zurich.* 41:383.

Overton, E. 1899. Ueber die allgemeinen osmotischen Eigenschaften der Zelle, ihre vermutlichen Ursachen und ihre Bedeutung fur die Physiologie. *Vjschr. Naturforsch. Ges. Zurich.* 44:88.

Pace, R. J., and S. I. Chan. 1982. Molecular motions in lipid bilayers. III. Lateral and transverse diffusion in bilayers. *J. Chem. Phys.* 76: 4241–4247.

Paula, S., A. G. Volkov, A. N. V. Hoek, T. H. Haines, and D. W. Deamer. 1996. Permeation of protons, potassium ions, and small polar molecules through phospholipid bilayers as a function of membrane thickness. *Biophys. J.* 70:339–348.

Peters, R., and K. Beck. 1983. Translational diffusion in phospholipid monolayers measured by fluorescence microphotolysis. *Proc. Natl. Acad. Sci. USA.* 80:7183–7187.

Piette, L. H., and W. A. Anderson. 1959. Potential energy barrier determination for some alkyl nitrates by nuclear magnetic resonance. *J. Chem. Phys.* 30:899–908.

Sada, E., S. Katoh, M. Terashima, H. Kawahara, and M. Katoh. 1990. Effects of surface charges and cholesterol content on amino acid permeabilities of small unilamellar vesicles. *J. Pharm. Sci.* 79:232–235.

Schindler, H., and J. Seelig. 1975. Deuterium order parameters in relation to thermodynamic properties of a phospholipid bilayer. A statistical mechanical interpretation. *Biochemistry.* 14:2283–2287.

Schnitzer, J. E. 1988. Analysis of steric partition behavior of molecules in membranes using statistical physics. Application to gel chromatography and electrophoresis. *Biophys. J.* 54:1065–1076.

Seelig, A., and J. Seelig. 1974. The dynamic structure of fatty acyl chains in a phospholipid bilayer measured by deuterium magnetic resonance. *Biochemistry.* 13:4839–4845.

Simon, S. A., and T. J. McIntosh. 1984. Interdigitated hydrocarbon chain packing causes the biphasic transition behavior in lipid/alcohol suspensions. *Biochim. Biophys. Acta.* 771:169–172.

Stein, W. D. 1986. Transport and Diffusion Across Cell Membranes. Academic Press, Inc., Orlando, FL.

Subczynski, W. K., W. E. Antholine, J. S. Hyde, and A. Kusumi. 1990. Microimmiscibility and three-dimensional dynamic structures of phosphatidylcholine-cholesterol membranes: translational diffusion of a copper complex in the membrane. *Biochemistry.* 29:7936–7945.

Subczynski, W. K., and J. S. Hyde. 1983. Concentration of oxygen in lipid bilayers using a spin-label method. *Biophys. J.* 41:283–286.

Todd, A. P., R. J. Mehlhorn, and R. I. Macey. 1989a. Amine and carboxylate spin probe permeability in red cells. *J. Membr. Biol.* 109:41–52.

Todd, A. P., R. J. Mehlhorn, and R. I. Macey. 1989b. Amine spin probe permeability in sonicated liposomes. *J. Membr. Biol.* 109:53–64.

Trauble, H. 1971. The movement of molecules across lipid membranes: a molecular theory. *J. Membr. Biol.* 4:193–208.

Turnbull, D., and M. H. Cohen. 1970. On the free-volume model of the liquid-glass transition. *J. Chem. Phys.* 52:3038–3041.

Vaz, W. L. C., R. M. Clegg, and D. Hallmann. 1985. Translational diffusion of lipids in liquid crystalline phase phosphatidylcholine multibilayers. A comparison of experiment with theory. *Biochemistry.* 24:781–786.

Vist, M. R., and J. H. Davis. 1990. Phase equilibria of cholesterol/dipalmitoylphosphatidylcholine mixtures: ^{2}H nuclear magnetic resonance and differential scanning calorimetry. *Biochemistry.* 29:451–464.

Vrentas, J. S. 1977. Diffusion in polymer-solvent systems. I. Reexamination of the free-volume theory. *J. Polym. Sci.* 15:403–416.

Walter, A., and J. Gutknecht. 1986. Permeability of small nonelectrolytes through lipid bilayer membranes. *J. Membr. Biol.* 90:207–217.

Warner, M. 1980. Interaction energies in nematogens. *J. Chem. Phys.* 73:5874–5883.

Wolfe, D. H., and H. L. Brockman. 1988. Regulation of the surface pressure of lipid monolayers and bilayers by the activity of water: derivation and application of an equation of state. *Proc. Natl. Acad. Sci. USA.* 85:4285–4289.

Xiang, T.-X. 1993. A computer simulation of free volume distributions and related structural properties in a model lipid bilayer. *Biophys. J.* 65: 1108–1120.

Xiang, T.-X., and B. D. Anderson. 1994a. Molecular distributions in lipid bilayers and other interphases: a statistical mechanical theory combined with molecular dynamics simulation. *Biophys. J.* 66:561–573.

Xiang, T.-X., and B. D. Anderson. 1994b. The relationship between permeant size and permeability in lipid bilayer membranes. *J. Membr. Biol.* 140:111–121.

Xiang, T.-X., and B. D. Anderson. 1994c. Substituent contributions to the permeability of substituted *p*-toluic acids in lipid bilayer membranes. *J. Pharm. Sci.* 83:1511–1518.

Xiang, T.-X., and B. D. Anderson. 1995a. Development of a combined NMR paramagnetic ion-induced line-broadening/dynamic light scattering method for permeability measurements across lipid bilayer membranes. *J. Pharm. Sci.* 84:1308–1315.

Xiang, T.-X., and B. D. Anderson. 1995b. Phospholipid surface density determines the partitioning and permeability of acetic acid in DMPC: cholesterol bilayers. *J. Membr. Biol.* 148:157–167.

Xiang, T.-X., X. Chen, and B. D. Anderson. 1992. Transport methods for probing the barrier domain of lipid bilayer membranes. *Biophys. J.* 63:78–88.